PREDICTIVE ANALYSES AND EXPERIMENTAL VALIDATIONS OF EFFECTIVE ELASTIC PROPERTIES OF 2D AND 3D WOVEN COMPOSITES

Stepan V. Lomov, Dmitry S. Ivanov, Ignaas Verpoest,

K.U. Leuven , Dept. MTM, Kasteelpark Arenberg, 44, B-3001, Leuven, Belgium
Stepan.Lomov@mtm.kuleuven.be

Alexander E. Bogdanovich, Dmitri Mungalov,

3TEX, Inc., 109 MacKenan Drive Cary, NC 27511, USA

Masaru Zako, Tetutsei Kurashiki, Hiroaki Nakai

Department of Management of Industry and Technology, Osaka University, 2-1, Yamadaoka, Suita, Osaka, 565-0871, Japan

ABSTRACT

The paper presents comparative experimental study and theoretical predictions of effective elastic properties of a single-layer 3D woven fabric E-glass/epoxy composite and its four-layer plain weave counterpart. Both composites were fabricated by VARTM in identical laboratory conditions using same fiber and resin materials. Both composites have identical preform areal density, very close fibre volume fraction and sample thickness. The predictions were performed using several methods of different complexity – Orientation Averaging, Method of Inclusions, finite element analysis and 3D MOSAIC analysis. Theoretical results are compared with experimental data obtained from in-plane tensile tests in warp, fill and off-axis $\pm 45°$ directions. Results obtained with the method of inclusions are in a close agreement with experimental data for both 2D and 3D woven composites, including properties in the off-axis loading. Orientation Averaging gives slightly lower elastic moduli in both in-plane fiber directions of 3D woven fabric. Finite element analysis, performed for the 2D weave laminate only, shows very good agreement with experimental data for the in-plane effective elastic properties. 3D MOSAIC analysis, performed for the 3D weave composite only, shows excellent agreement with experimental results for the in-plane elastic moduli and Poisson's ratio.

1 INTRODUCTION

Predictions of preform geometry and mechanical properties of composites reinforced with 3D woven fabrics is on a high demand [1, 2]. Methodologically adequate and computationally efficient predictive analysis tools would open new ways toward optimising the fabric architectures, using in full the opportunities offered by the available automated and well controlled 3D weaving processes and machines [3]. Further on, the availability of analysis tools capable of predicting mechanical properties and structural responses of 3D woven composites is very important for engineers and

designers implementing this class of materials in practice. Various analysis tools are currently available, see review in [1], however very little has yet been reported on mutual comparison of numerical results and their validation by experimental data. This paper is among initial efforts to address this important research problem. The paper presents a comparison of numerical analysis results for effective elastic properties of a representative 3D woven E-glass/epoxy composite and its 2D woven counterpart, and the respective experimental validations. The unique feature of this research work is that the compared four-layer 2D weave and single-layer 3D weave composites have equivalent areal weight of fabric preform; they were fabricated in the same lab by the same personnel using same fiber and resin systems, same VARTM equipment and processing regime.

The analysis reported here was performed by several methods of increasing complexity: Orientation Averaging introduced in [4] (see details and references in [5]), Method of inclusions [6-9], Finite Element Meso-model [10, 11], and multi-scale 3D MOSAIC model [1, 12, 13]. The effective elastic properties predicted by all these analysis methods are compared to mechanical test data. The ability of each analysis method used here to predict different mechanical properties is summarized in Table 1.

Table 1 The ability of modelling methods to predict different mechanical properties

Analysis method	Effective elastic constants	Failure initiation	Ultimate failure/strength via progressive failure
Orientation Averaging	Yes	No	No
Method of Inclusions	Yes	No	No
3D MOSAIC	Yes	Yes	Yes
3D Finite Element	Yes	Yes	Yes

This paper focuses on the elastic properties. The initial failure, progressive damage and ultimate failure/strength predictions, together with their experimental validations, will be reported elsewhere.

2 MATERIALS

Composite material samples were fabricated in a vacuum bag with Dow Derakane 8084 Epoxy-Vinyl Ester resin. Two kinds of fabric preform were used: (1) single layer, 96 oz/yd^2 (3255 g/m^2) areal density, 3D orthogonal weave made from E-glass fibres and (2) a stack of four layers of 24 oz/yd^2 (815 g/m^2, in total 3260 g/m^2) plain weave made from same E-glass fibres. Both preforms have identical areal weight and, in a free state, their thicknesses were very close, ~2.8 mm. It is worth mentioning that 24 oz/yd^2 areal density woven roving is a widely used E-glass fabric produced by several companies, while 96 oz/yd^2 E-glass 3D orthogonal weave is one of most popular 3TEX's commercial products.

The 96 oz/yd^2 3D weave was made of PPG Hybon 2022 E-glass roving in warp, fill and Z directions; it contains 3 warp and 4 fill layers. Warp layers #1 and #3 use 218 yield (2275 tex) roving, while layer #2 uses 450 yield (1100 tex) roving (all layers have 7 ends/inch or 2.76 ends/cm insertion frequency). All fill layers use 330 yield (1470 tex) roving with 6.7 picks/inch (2.64 picks/cm) insertion. Z-directional reinforcement uses 1800 yield (276 tex) roving with 7 ends/inch (2.76 ends/cm) insertion frequency. This construction results in ~49% warp-, ~49% fill- and ~2% Z-fiber content per preform volume. The internal fiber architecture of the 3D reinforcement was studied earlier in [14] using micro-CT and optical microscopy; some results are shown in Figure 1.

The plain weave was made of 218 yield (2275 tex) PPG Hybon 2022 E-glass roving in both warp and fill directions; the respective insertions were 5 ends/inch (1.95 ends/cm) in warp and 4.1 picks/inch (1.60 picks/cm) in fill. Note the difference between fiber amounts in warp and fill directions, which asked to alternate fabric layer orientation in the 4-layer preform.

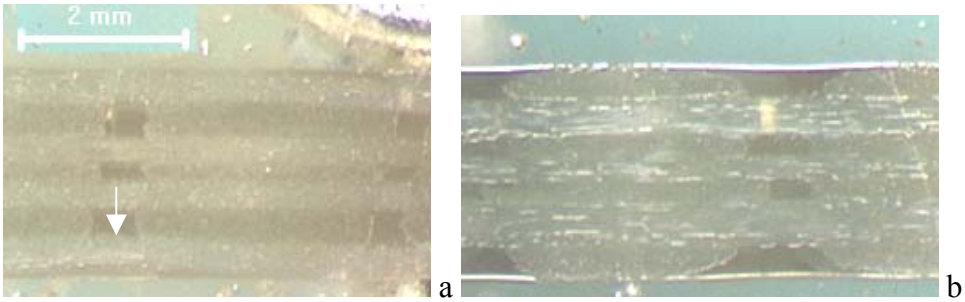

Figure 1 Cross-section of 3D woven fabric composite along fill (a) and warp (b). Note compression of the Z-yarns and slight crimp of the outer fill (arrow)

In-plane dimensions of the preforms were identical, 127 cm length and 43 cm width. In case of 2D weave the fill-directional yarns in two outer fabric layers coincided with the length direction, while in two inner fabric layers fill yarns were oriented in the width direction. Same equipment and materials were used for VARTM process in both cases, and the processing parameters were kept as close as possible.

3 EXPERIMENTAL

Following experimental methodology described in [15, 16], the performed studies provided:

- Stress-strain curves under tensile loading;
- Acoustic emission (AE) event accumulation and cumulative AE energy;
- Full-field surface strain-mapping (SM);

Tensile Tests. Tensile tests were performed on a standard testing machine Instron 4505 with test speed 5 mm/min. The samples were cut out of the composite plates in three characteristic directions: (1) warp, (2) fill and (3) bias 45°. The error in strains given by the displacements of the grips due to the machine compliance was eliminated by the optical extensometry and the true values of the strain in the centre of the sample were used in the final results.

Acoustic Emission Acoustic emission (AE) is the detection of transient stress waves caused in a material by a fast release of strain energy in that material. AE system AMSY-5 (Vallen Systems Gmbh) was used here. Two AE sensors were situated at the boundaries of the gauge length region. Signals that occur outside of the sensors are filtered out by the system. The energy of AE events was registered and the dependency of cumulative energy of AE events vs. tensile strain was plotted. Change in the rate of AE event accumulation indicates initiation of the damage and a switch to another damage mechanism.

Strain Mapping Strain mapping is a system of measuring surface strain using correlation of digital images taken on a sample during loading. The Vic2D software (LIMESS Messtechnik und Software GmbH) was used here. The samples were first painted with a black and white random speckle pattern to give a unique pattern of the examined surface. As the tensile test proceeds, the system takes subsequent images and

analyses them in comparison to the initial image, thus allowing one to determine local displacement and strain values. The produced detailed surface strain field maps are used (1) as an optical extensometer (after averaging over the centre region of the sample) and (2) for gaining detailed information of strain distribution and validating computational modelling and analysis tools (analysis of the strain fields will be presented in future publications).

The results of the measurements are summarised in Table 2. The theoretical work reported in this paper focuses on elastic behaviour of the composites, up to a damage initiation. Numerical analysis of progressive damage, strength and ultimate strain will be reported in future publications.

Table 2 Results of tensile experiments

Parameter	3D weave composite, $V_f = 49.3\%$			2D weave composite, $V_f = 52.4\%$	
	warp	fill	bias	warp/fill	bias
Young's moduli, GPa	24.5±1.2	25.1±2.3	12.9±0.5	26.0±1.5	12.3±0.4
Poisson's ratios	0.141±0.071	0.126±0.093	0.502±0.21	0.264±0.148	0.61±0.148
Damage initiation strain, %	0.43±0.04	0.37±0.06	0.63±0.07	0.26±0.04	1.23±0.35
Strength, MPa	429±34	486±5	124±5	413±4	109±6
Ultimate strain, %	2.74±0.29	3.33±0.27	14.1±0.4	2.38±0.02	9.7±0.4

Note: "±" refers to the standard deviation in 9 tests (Young's moduli, Poisson's ratio, damage initiation strain) and 3 tests (strength, ultimate strain)

4 GEOMETRICAL MODELS OF THE UNIT CELL

Geometrical models of 2D weave and 3D weave unit cells and their composites were built by TU Leuven using WiseTex software [7-9] and by 3TEX using SolidWorks® and 3D MOSAIC software. The care was taken to preserve in the models the parameters of the composites and reinforcements, which are well controlled and measurable, such as total fibre volume fraction, partial fiber volume fractions in warp and fill directions, areal density of the fabrics, ends/picks spacing, and composite thickness.

4.1 Plain weave laminated composite

The model of the plain woven fabric laminate (0°/90°/90°/0° orientation of the layers, Figure 2a) is built based on the following data obtainable without cross-sectioning of the composite plate (Table 3):

- Thickness of the composite plate, which was measured to be 2.45±0.08 mm. This value gives the fibre volume fraction of the plate 52.4% and the average thickness of the layers 0.612 mm. The latter does not account for the (unknown) nesting of the yarns.
- Spacing of the warp and weft yarns (ends/picks count, see Section 2 above), given by the fabric specifications and verified by the direct measurements on the composite plate. These values were directly used in WiseTex model.
- Thickness of the warp and weft yarns was assumed to be 0.3 mm, which, together with the crimp of the yarn calculated using WiseTex (slightly different for warp and weft due to the different spacing), produced the thickness of one layer equal to the measured value 0.612 mm. The areal density of the fabric in WiseTex model is 809 g/m^2 and the overall fibre volume fraction is 52.0%, which correspond to the specified and measured values.

– Width of the warp and weft yarns was estimated using the images of the surface of the plate as 5.1 mm (Figure 2b). This value gives fibre volume fraction inside the yarns of 75%, which corresponds to the typical values observed for woven fabrics [17].

– The shape of the warp and fill yarn cross section was assumed to be elliptical and was kept constant.

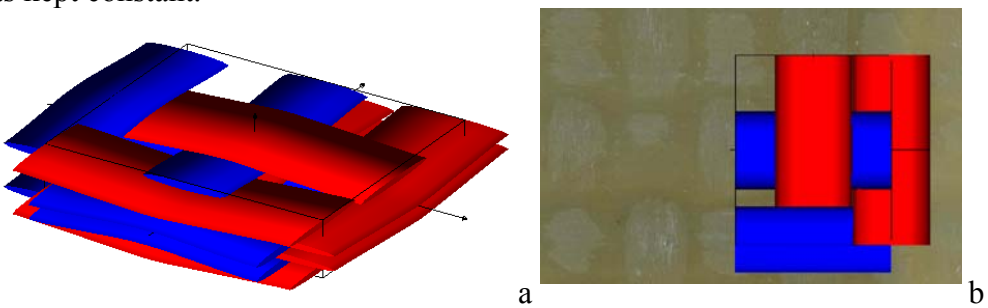

a b

Figure 2 Geometrical model of the plain weave laminate: (a) 3D image of the laminate; (b) comparison of the model of one layer and the photo of the surface of the composite plate

Table 3 Parameters of the geometrical model: 2D plain weave composite

INPUT data	*Value*	*CALCULATED data*	*Value*
Ends/picks count, 1/cm	1.95 / 1.60	Fabric areal density, g/m^2	809
Yarn linear density, tex	218	Layer thickness	0.612
Yarn width, mm	5.1	Fibre volume fraction, %	54.0
Yarn thickness, mm	0.3	Fibre volume fraction in yarns, %	74.5
Cross-section shape	ellipse	Warp/fill crimp, %	0.1 / 0.2

4.2 WiseTex model of 3D weave single layer composite

The *WiseTex* model of 3D woven fabric and composite is described in Figure 3a and Table 4. It is based on the fabric specifications and measurements on the cross-sections of the composite plate. The dimensions of the yarns in the composite are slightly different from the values for dry fabric, reported earlier in [14]. The most important difference is the low thickness of the Z-yarns and slight crimp of the fill in the outer layers (see Figure 1a).

Table 4 Parameters of the geometrical model: 3D woven composite

Parameter	*Input Data*
Ends/Z/picks count, 1/cm/layer	2.76 / 2.76 / 2.64
Yarn linear density, tex (warp in layers/Z/fill)	2275, 1100, 2275 / 276 / 1470
Yarn width, mm (warp in layers / Z / fill)	3.32, 3.26, 3.32 / 0.58 / 3.16
Yarn thickness, mm (warp in layers / Z / fill)	0.42, 0.22, 0.42 / 0.24 / 0.31
Cross-section shape	rectangle
Calculated Data	
Fabric areal density, g/m^2	3244
Layer thickness	2.60
Fibre volume fraction (VF), %	49.0
V_f in yarns, % (warp in layers / Z / fill)	64, 61, 64 / 78 / 59
Fill crimp in the outer layers, %	2.1

The shape of Z-yarns is simplified in the WiseTex model: the dimensions of the cross-section are kept constant along the yarn. This leads to interpenetration of the yarn volumes, which prevented building an FE model for this fabric in the current stage of computational work. The accepted dimensions of the Z-yarns are based on measurements of its cross-section over fill, on the surface of the fabric, in the most

compressed state (note also high fibre volume fraction inside the Z-yarn). These dimensions fit the composite sample thickness and hence preserve the correct overall fibre volume fraction.

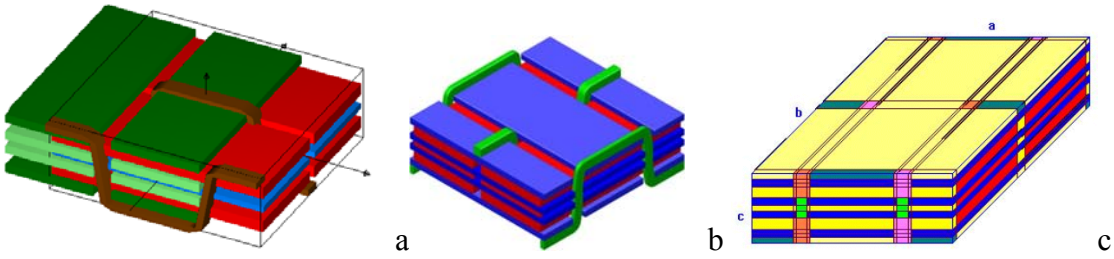

Figure 3 WiseTex (a) and 3TEX's (b) geometrical models of 3D woven fabric and (c) 3D MOSAIC model of 3D woven composite

4.3 3TEX's model of 3D weave single layer composite

The other geometric model of the same 3D woven fabric unit cell, shown in Figure 3b, has been independently generated by 3TEX using their computational tools. The yarn insertion parameters, such as ends/cm and picks/cm counts, yarn linear density and rectangular cross-sectional shapes of all yarns used in this model, are the same as in Table 4. The yarn cross-sectional dimensions are slightly different. All warp yarns within the unit cell have same length 3.791 mm, same width 3.208 mm but different thickness. For the top and bottom warp layers this is 0.466 mm, while for the middle layer 0.226 mm. The top and bottom fill yarns have length 3.629 mm, width 3.160 mm and thickness 0.313 mm, while the two middle fill yarns have length 3.629 mm, width 3.360 mm and thickness 0.294 mm. Z-yarn has 0.431 mm dimension in x direction, 0.420 mm in y direction and length 2.371 mm. Total thickness of the fabric unit cell without "Z-crowns" (painted green in Figure 3b) is 2.371 mm and with Z-crowns it is 3.234 mm. When the preform was compressed in vacuum bag, its thickness got intermediate value between the two above, namely 2.602 mm, which was measured on the final composite.

5 ORIENTATION AVERAGING AND INCLUSIONS MODELS

All the calculations were done using the following data for isotropic materials of E-glass fibre and Derakane 8084 Epoxy-Vinyl Ester matrix: Young's modulus 72.5 and 2.9 GPa, Poisson's ratio 0.23 and 0.35. Table 5 shows homogenised properties of the resin-impregnated yarns (treated as transversely isotropic unidirectional composites), calculated using Mori-Tanaka method and further utilized in the analysis of 2D weave and 3D weave composites performed by KU Leuven. Index "1" refers to the fibre direction, indices "2,3" – to the transverse directions. The calculations were performed using *TexComp* software, which directly imports the *WiseTex* geometry, subdivides the yarns into segments (20 per crimp interval on the yarns), and then performs homogenisation using iso-strain assumption (Stiffness Averaging) or Mori-Tanaka method. Note that all calculations are based on the same *WiseTex* model and account for the crimp of the yarns. 3TEX used identical $V_f = 67.7\%$ for all yarns (warp, fill and Z) in their analysis of 3D weave composite. The respective effective elastic characteristics were predicted by Stiffness Averaging (SA) method; they are also included in Table 5. Note that the micromechanics incorporated in 3TEX's effective elastic property predictions of UD composites is different from the one used by KU Leuven, thus the results for the same V_f value would not be necessarily identical.

Table 5 Homogenised properties of the yarns obtained by Mori-Tanaka (M-T) and SA methods

UD composites used in	V_f, %	E_1, GPa	E_2, E_3, GPa	ν_{12} , ν_{13}	ν_{23}	G_{12}, G_{13}, GPa	G_{23}, GPa
2D plain weave	74.5	54.4	14.7	0.255	0.422	5.91	5.18
3D, warp 2275 tex	64.1	47.2	10.8	0.266	0.440	4.24	3.73
3D, warp 1100 tex	60.1	44.5	9.7	0.271	0.445	3.79	3.35
3D, Z 276 tex	78.0	56.8	16.7	0.252	0.414	6.73	5.9
3D, fill 1470 tex	59.1	43.7	9.44	0.272	0.447	3.69	3.26
3D, warp fill and Z (3TEX data)	67.7	50.0	11.9	0.314	0.441	4.68	4.12

6 3-D FINITE ELEMENT AND 3D MOSAIC MODELS

6.1 FE analysis of 2D plain weave composite laminate

FE model for unit cell of the 2D plain weave composite was built and solved using *MeshTex/SACOM* software [10, 11], which directly imports geometrical model of one layer of the fabric from *WiseTex*. In order to mesh the unit cell, *MeshTex* inserts thin (0.005 mm) layers of matrix in between the warp and fill yarns and on the surface of the unit cell. The resulting V_f of the unit cell is hence slightly decreased to 47.2% (52.0% in *WiseTex* model). The unit cell is unbalanced, hence it is difficult to impose correct boundary conditions on the laminate model (Figure 2a). Because of these two factors, the following calculation route was adopted:

1. Perform FE homogenisation of the unit cell using periodic boundary conditions in all the directions
2. Scale elastic properties to fibre volume fraction 52.0%
3. Calculate homogenised laminate properties using Classical Laminate Theory with properties of lamina calculated as above

Use of periodic boundary conditions in thickness direction may be questioned as the plate has only four plies and free surfaces are not far from the middle of the plate. However, the overestimation of the stiffness, connected with that, is believed to compensate the underestimation of the stiffness resulting from the neglecting of the nesting of the layers.

6.2 3D MOSAIC analysis of 3D woven composite

3D MOSAIC model of the 3D weave composite unit cell was built on the basis of the fabric geometry model shown in Figure 3b. The developed model is shown in Figure 3c. This is quite a complex mosaic body which contains seven distinct composite materials: (1) UD warp yarn (red), (2) UD fill yarn (blue), (3) UD Z yarn in x direction (dark green), (4) UD Z yarn in z direction (light green), (5) pure matrix (yellow), (6) monoclinic composite (MC) having clockwise inclined Z yarn smeared with matrix (brown), and (7) MC having counter clockwise inclined Z yarn smeared with matrix (purple). The latter two materials, monoclinic in nature, are characterized by 13 independent elastic constants. The appearance of these seven homogenized materials in the 3D MOSAIC model of Figure 3c should be clear from respective geometric model of Figure 3b.

The procedures required to perform 3-D stress-strain analysis of mosaic structure shown in Figure 3c and compute its effective elastic properties were described in detail and illustrated on practical examples in [1]. Briefly, three coupled boundary value problems have to be formulated and solved in order to obtain effective Young's moduli E_1, E_2 and E_3 and Poisson's ratios ν_{12}, ν_{13} and ν_{23}. Another three independent boundary value

problems have to be formulated and solved to obtain shear moduli G_{12}, G_{13} and G_{23}. These problems can be solved under two types of boundary conditions: applied displacements (strains) or applied stresses. The results would provide a "fork" between the upper and lower bounds of each effective elastic constant, see illustrative example in [13]. Here we will only present results for the case of displacement boundary conditions applied to mosaic body. Another important notice is that in this analysis approach the convergence of computed displacement, strain and stress fields can be studied by either increasing degree of Bernstein basis functions, or by discretizing material bricks in Figure 3c into smaller computational elements, see [1, 12]. Numerical results presented in the next section correspond to converged values of all effective elastic constants.

7 DISCUSSION OF RESULTS

Table 6 shows numerical results obtained for effective elastic properties of the studied 2D weave and 3D weave composites using iso-strain variant of Orientation Averaging (OA), Mori-Tanaka (M-T), FEA and 3D MOSAIC in their mutual comparison and also in comparison with respective experimental results.

The comparison shows that for 2D woven composite, the OA, M-T and FE analyses give results very close to the experimental data for all the considered engineering constants. All theoretical values of Poisson's ratio ν_{12} are consistently lower (about two times) than the average experimental value, but they are near the edge of the experimental scatter, which is very large for this characteristic. FE gives slightly better agreement with experimental value for ν_{12}.

Table 6 Experimental and theoretical results for effective elastic properties of 2D weave and 3D weave composites

Property	2D plain weave 0/90/90/0 composite				3D weave composite				
	exp	OA*	M-T	FE	**exp**	OA*	M-T	OA**	3D MOSAIC
E_1, GPa	**26.0**±1.5	25.1	25.4	25.2	**24.3**±1.2	22.7	24.17	22.1	23.0
E_2, GPa	**26.0**±1.5	25.1	25.4	25.2	**25.1**±2.34	22.8	24.21	22.3	24.7
E_3, GPa	n/a	12.2	8.63	8.55	n/a	10.1	9.11	9.64	9.37
G_{12}, GPa	n/a	4.4	4.2	4.5	n/a	3.38	3.22	2.87	n/a
ν_{12}	**0.264**±0.148	0.118	0.117	0.128	**0.141**±0.071	0.109	0.161	0.120	0.137
ν_{13}	n/a	0.372	0.396	0.402	n/a	0.377	0.370	0.384	0.404
ν_{23}	n/a	0.372	0.396	0.402	n/a	0.380	0.368	0.383	0.397
E_{45^o}, GPa	**12.2**±0.4	13.6	13.0	n/a	**12.9**±0.5	10.7	10.4	n/a	n/a
G_{45^o}, GPa	n/a	11.2	11.4	n/a	n/a	10.3	10.8	n/a	n/a
ν_{45^o}	**0.610**±0.148	0.524	0.549	n/a	**0.502**±0.21	0.581	0.618	n/a	n/a

Notes: "±" – standard deviation in 9 tests;
OA* - KU Leuven version and OA** - 3TEX version of Orientation Averaging analysis

For 3D woven composite, the two versions of OA analysis were used, and their results are shown in Table 6 separately. Both of them provide considerably lower values for E_1, E_2 and ν_{12} than experimental data. The differences in the results provided by these two OA approaches can be attributed to the different micromechanics used and/or to possible slight difference in fiber volume fraction assumed in each analysis. The M-T results are considerably closer to experimental data (especially for E_1), however it overestimates ν_{12}. The 3D MOSAIC results show best agreement with experimental value for E_2 and ν_{12} , better agreement for E_1 than both OA analyses, though there is a larger deviation for this characteristic than in the M-T analysis. Also note that predictions provided by M-T, 3D MOSAIC and OA for the other engineering constants,

namely E_3, ν_{13}, and ν_{23}, are in a good mutual agreement. There are no presently available experimental data for these elastic constants.

8 CONCLUSIONS

Several different types of analysis have been implemented in this work for predicting effective elastic properties of 2D woven four-ply laminated composite and 3D woven single-ply composite made of E-glass fiber and Derakane 8084 Epoxy-Vinyl Ester matrix. The methods used here are of a very different complexity, from Orientation Averaging, to Method of Inclusions, to 3-D Finite Element and 3D MOSAIC. The results have been compared with experimental data obtained from the in-plane tensile tests in the warp, fill and off-axis 45° directions for both composites. The comparison shows that the Method of Inclusions enables for sufficiently accurate predictions of the in-plane effective elastic properties for both 2D and 3D woven composites, including properties in the off-axis loading. The Orientation Averaging method performs well in the case of 2D woven composite, but is less accurate in the case of 3D woven composite. The Finite Element analysis performed for 2D woven composite only, showed very good agreement with experimental data, yet its results are very close to the ones obtained from the Orientation Averaging and Method of Inclusions. 3D MOSAIC analysis was performed for 3D woven composite only; it showed best agreement with experimental data for the fill-directional modulus and in-plane Poisson's ratio.

It has to be pointed out again that the methods of Orientation Averaging and Inclusions have been originally developed for effective elastic property predictions. They do not provide stress/strain fields and cannot be used for failure initiation, progression and strength predictions. Contrary to that, Finite Element and Variational analysis approaches, represented here by one specific 3-D finite element type and by 3D MOSAIC model, are not primarily aimed for effective elastic property predictions. Their computational expense is incomparably higher compared to the other two aforementioned methods. Hence, their application is advisable only in those cases when those much simpler methods produce obviously inadequate or inaccurate results.

ACKNOWLEDGEMENT

The work reported here was partially supported at K.U. Leuven by PhD grant of D.S. Ivanov (the K.U. Leuven Research Council)

REFERENCES

1. Bogdanovich, A.E., *Multi-scale modeling, stress and failure analyses of 3-D woven composites.* Journal of Materials Science, 2006. **41**(20): p. 6547-6590.
2. Bogdanovich, A.E. *Advancements in manufacturing and applications of 3D woven preforms and composites*. in *The 16th International Conference on Composites Materials (ICCM-16)*. 2007. Kyoto.
3. Mohamed, M.H., A.E. Bogdanovich, L.C. Dickinson, J.N. Singletary, and R.B. Lienhart, *A new generation of 3D woven fabric preforms and composites.* SAMPE Journal, 2001. **37**(3): p. 8-17.
4. Kregers, A.F. and Y.G. Melbardis, *Determination of the deformability of three-dimensionally reinforced composites by the stiffness averaging method.* Polymer Mechanics, 1978. **14**: p. 3-8.
5. Bogdanovich, A.E. and C.M. Pastore, *Mechanics of Textile and Laminated Composites*. 1996, London: Chapman and Hall.

6. Huysmans, G., I. Verpoest, and P. Van Houtte, *A poly-inclusion approach for the elastic modelling of knitted fabric composites.* Acta Materials, 1998. **46**(9): p. 3003-3013.

7. Lomov, S.V., G. Huysmans, Y. Luo, A. Prodromou, I. Verpoest, and A.V. Gusakov. *Textile Geometry Preprocessor for meso-mechanical and permeability modelling of textile composites*. in *9th European Conference on Composite Materials (ECCM-9)*. 2000. Brighton: IOM Communications.

8. Lomov, S.V., G. Huysmans, Y. Luo, R. Parnas, A. Prodromou, I. Verpoest, and F.R. Phelan, *Textile Composites: Modelling Strategies.* Composites part A, 2001. **32**(10): p. 1379-1394.

9. Lomov, S.V., I. Verpoest, E. Bernal, F. Boust, V. Carvelli, J.-F. Delerue, P. De Luka, L. Dufort, S. Hirosawa, G. Huysmans, S. Kondratiev, B. Laine, T. Mikolanda, H. Nakai, C. Poggi, D. Roose, F. Tumer, B. van den Broucke, B. Verleye, and M. Zako, *Virtual textile composites software Wisetex: integration with micro-mechanical, permeability and structural analysis*, in *Proceedings of the 15th International Conference on Composite Materials (ICCM-15)*. 2005: Durban. p. CD edition.

10. Lomov, S.V., D.S. Ivanov, I. Verpoest, M. Zako, T. Kurashiki, H. Nakai, and S. Hirosawa *Meso-FE modelling of textile composites: Road map, data flow and algorithms.* Composites Science and Technology, 2007. **67**: p. 1870-1891.

11. Verpoest, I. and S.V. Lomov, *Virtual textile composites software Wisetex: integration with micro-mechanical, permeability and structural analysis.* Composites Science and Technology, 2005. **65**(15-16): p. 2563-2574.

12. Bogdanovich, A.E., *Three-dimensional variational theory of laminated composite plates and its implementation with bernstein basis functions.* Computer Methods in Applied Mechanics and Engineering, 2000. **185**(2-4): p. 279-304.

13. Bogdanovich, A.E. *Multiscale predictive analysis of 3D woven composites*. in *35th International SAMPE Technical Conference*. 2003. Dayton, Ohio.

14. Desplentere, F., S.V. Lomov, D.L. Woerdeman, I. Verpoest, M. Wevers, and A. Bogdanovich, *Micro-CT Characterization of variability in 3D textile architecture.* Composites Science and Technology, 2005. **65**: p. 1920-1930.

15. Lomov, S.V., D.S. Ivanov, T. Truong Chi, I. Verpoest, F. Baudry, K. Vanden Bosche, and H. Xie, *Experimental methodology of study of damage initiation and development in textile composites in uniaxial tensile test.* Composites Science and Technology, in print.

16. Lomov, S.V., D.S. Ivanov, I. Verpoest, M. Zako, T. Kurashiki, H. Nakai, J. Molimard, and A. Vautrin, *Full field strain measurements for validation of meso-FE analysis of textile composites.* Composites part A, in print.

17. Koissin, V., D.S. Ivanov, S.V. Lomov, and I. Verpoest, *Fibre distribution inside yarns of textile composite: geometrical and FE modelling*, in *Proceedings of the 8th International Conference on Textile Composites (TexComp-8)*. 2006: Nottingham. p. CD edition.